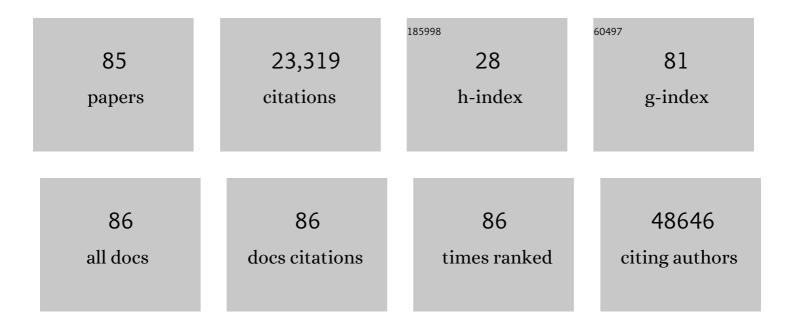
## Marco Cecchini

List of Publications by Year in descending order

Source: https://exaly.com/author-pdf/7031495/publications.pdf Version: 2024-02-01



#	Article	IF	CITATIONS
1	Bio-inspired nanoparticles as drug delivery vectors. , 2022, , 499-528.		0
2	Chronic lithium administration in a mouse model for Krabbe disease. JIMD Reports, 2022, 63, 50-65.	0.7	7
3	Detection of Oenological Polyphenols via QCM-D Measurements. Nanomaterials, 2022, 12, 166.	1.9	6
4	Surfaceâ€Acousticâ€Wave (SAW) Induced Mixing Enhances the Detection of Viruses: Application to Measles Sensing in Whole Human Saliva with a SAW Labâ€Onâ€aâ€Chip. Advanced Functional Materials, 2022, 32, .	7.8	19
5	Measuring Molecular Diffusion in Dynamic Subcellular Nanostructures by Fast Raster Image Correlation Spectroscopy and 3D Orbital Tracking. International Journal of Molecular Sciences, 2022, 23, 7623.	1.8	0
6	Photoresponse of the AlN-Based SAW Device on Polymeric and Silicon Substrates. IEEE Sensors Journal, 2021, 21, 9675-9681.	2.4	9
7	Ultra-high-frequency (UHF) surface-acoustic-wave (SAW) microfluidics and biosensors. Nanotechnology, 2021, 32, 312001.	1.3	26
8	Acoustic streaming of microparticles using graphene-based interdigital transducers. Nanotechnology, 2021, 32, 375503.	1.3	6
9	Chitosan Micro-Grooved Membranes with Increased Asymmetry for the Improvement of the Schwann Cell Response in Nerve Regeneration. International Journal of Molecular Sciences, 2021, 22, 7901.	1.8	18
10	Atomistic simulations of gold surface functionalization for nanoscale biosensors applications. Nanotechnology, 2021, 32, 095702.	1.3	9
11	Visual System Impairment in a Mouse Model of Krabbe Disease: The Twitcher Mouse. Biomolecules, 2021, 11, 7.	1.8	7
12	An objective, principal-component-analysis (PCA) based, method which improves the quartz-crystal-microbalance (QCM) sensing performance. Sensors and Actuators A: Physical, 2020, 315, 112323.	2.0	10
13	Ultra-High-Frequency Love Surface Acoustic Wave Device for Real-Time Sensing Applications. IEEE Access, 2020, 8, 112507-112514.	2.6	8
14	Neuronal contact guidance and YAP signaling on ultra-small nanogratings. Scientific Reports, 2020, 10, 3742.	1.6	18
15	Polydimethylsiloxane (PDMS) irreversible bonding to untreated plastics and metals for microfluidics applications. APL Materials, 2019, 7, .	2.2	33
16	Chitosan films for regenerative medicine: fabrication methods and mechanical characterization of nanostructured chitosan films. Biophysical Reviews, 2019, 11, 807-815.	1.5	38
17	Capturing Metabolism-Dependent Solvent Dynamics in the Lumen of a Trafficking Lysosome. ACS Nano, 2019, 13, 1670-1682.	7.3	15
18	Lipid-Conjugated Rigidochromic Probe Discloses Membrane Alteration in Model Cells of Krabbe Disease. Biophysical Journal, 2019, 116, 477-486.	0.2	6

#	Article	IF	CITATIONS
19	Full-SAW Microfluidics-Based Lab-on-a-Chip for Biosensing. IEEE Access, 2019, 7, 70901-70909.	2.6	28
20	Dysregulated autophagy as a new aspect of the molecular pathogenesis of Krabbe disease. Neurobiology of Disease, 2019, 129, 195-207.	2.1	30
21	MICAL2 is expressed in cancer associated neo-angiogenic capillary endothelia and it is required for endothelial cell viability, motility and VEGF response. Biochimica Et Biophysica Acta - Molecular Basis of Disease, 2019, 1865, 2111-2124.	1.8	14
22	Quantitative Microproteomics Based Characterization of the Central and Peripheral Nervous System of a Mouse Model of Krabbe Disease. Molecular and Cellular Proteomics, 2019, 18, 1227-1241.	2.5	25
23	Brain-targeted enzyme-loaded nanoparticles: A breach through the blood-brain barrier for enzyme replacement therapy in Krabbe disease. Science Advances, 2019, 5, eaax7462.	4.7	43
24	The role of ubiquitin ligase E3A in polarized contact guidance and rescue strategies in UBE3A-deficient hippocampal neurons. Molecular Autism, 2019, 10, 41.	2.6	10
25	Tuning polymorphism in 2,3-thienoimide capped oligothiophene based field-effect transistors by implementing vacuum and solution deposition methods. Journal of Materials Chemistry C, 2018, 6, 5601-5608.	2.7	21
26	Peptide-based coatings for flexible implantable neural interfaces. Scientific Reports, 2018, 8, 502.	1.6	24
27	A Rayleigh surface acoustic wave (R-SAW) resonator biosensor based on positive and negative reflectors with sub-nanomolar limit of detection. Sensors and Actuators B: Chemical, 2018, 254, 1-7.	4.0	35
28	Surface-Acoustic-Wave (SAW)-Driven Device for Dynamic Cell Cultures. Analytical Chemistry, 2018, 90, 7450-7457.	3.2	34
29	Perfluoropolyether (PFPE) Intermediate Molds for High-Resolution Thermal Nanoimprint Lithography. Nanomaterials, 2018, 8, 609.	1.9	13
30	Cross-Linked Enzyme Aggregates as Versatile Tool for Enzyme Delivery: Application to Polymeric Nanoparticles. Bioconjugate Chemistry, 2018, 29, 2225-2231.	1.8	34
31	RP ARS reveals molecular spatial order anomalies in myelin of an animal model of Krabbe disease. Journal of Biophotonics, 2017, 10, 385-393.	1.1	17
32	Multiscale structured germanium nanoripples as templates for bioactive surfaces. RSC Advances, 2017, 7, 9024-9030.	1.7	11
33	Embryo development in dynamic microfluidic systems. Sensors and Actuators B: Chemical, 2017, 250, 525-532.	4.0	15
34	Neuregulin 1 functionalization of organic fibers for Schwann cell guidance. Nanotechnology, 2017, 28, 155303.	1.3	11
35	Hierarchical thermoplastic rippled nanostructures regulate Schwann cell adhesion, morphology and spatial organization. Nanoscale, 2017, 9, 14861-14874.	2.8	20
36	Self-Assembled InAs Nanowires as Optical Reflectors. Nanomaterials, 2017, 7, 400.	1.9	20

#	Article	IF	CITATIONS
37	Surface Acoustic Wave (SAW)-Enhanced Chemical Functionalization of Gold Films. Sensors, 2017, 17, 2452.	2.1	12
38	Nanotopography Induced Human Bone Marrow Mesangiogenic Progenitor Cells (MPCs) to Mesenchymal Stromal Cells (MSCs) Transition. Frontiers in Cell and Developmental Biology, 2016, 4, 144.	1.8	2
39	Ultrastructural Characterization of the Lower Motor System in a Mouse Model of Krabbe Disease. Scientific Reports, 2016, 6, 1.	1.6	20,953
40	Lithium improves cell viability in psychosineâ€treated MO3.13 human oligodendrocyte cell line via autophagy activation. Journal of Neuroscience Research, 2016, 94, 1246-1260.	1.3	33
41	Human mesenchymal stromal cell-enhanced osteogenic differentiation by contact interaction with polyethylene terephthalate nanogratings. Biomedical Materials (Bristol), 2016, 11, 045003.	1.7	16
42	<i>MICAL2</i> is a novel human cancer gene controlling mesenchymal to epithelial transition involved in cancer growth and invasion. Oncotarget, 2016, 7, 1808-1825.	0.8	55
43	Rapid and Controllable Digital Microfluidic Heating by Surface Acoustic Waves. Advanced Functional Materials, 2015, 25, 5895-5901.	7.8	88
44	Schwann Cell Contact Guidance versus Boundary Â <del>l</del> nteraction in Functional Wound Healing along Nano and Microstructured Membranes. Advanced Healthcare Materials, 2015, 4, 1849-1860.	3.9	37
45	RP-CARS: label-free optical readout of the myelin intrinsic healthiness. Optics Express, 2014, 22, 13733.	1.7	24
46	Interaction of leech neurons with topographical gratings: comparison with rodent and human neuronal lines and primary cells. Interface Focus, 2014, 4, 20130047.	1.5	19
47	Nanoliterâ€Droplet Acoustic Streaming via Ultra High Frequency Surface Acoustic Waves. Advanced Materials, 2014, 26, 4941-4946.	11.1	149
48	Microfluidic pumping through miniaturized channels driven by ultra-high frequency surface acoustic waves. Applied Physics Letters, 2014, 105, 074106.	1.5	46
49	Tubeless biochip for tailoring cell co-cultures in closed microchambers. Microelectronic Engineering, 2014, 124, 8-12.	1.1	0
50	Acoustofluidics and Whole-Blood Manipulation in Surface Acoustic Wave Counterflow Devices. Analytical Chemistry, 2014, 86, 10633-10638.	3.2	25
51	Interaction of SH Y5Y Cells with Nanogratings During Neuronal Differentiation: Comparison with Primary Neurons. Advanced Healthcare Materials, 2014, 3, 581-587.	3.9	46
52	Tubeless biochip for chemical stimulation of cells in closed-bioreactors: anti-cancer activity of the catechin–dextran conjugate. RSC Advances, 2014, 4, 35017-35026.	1.7	3
53	Microstructured polydimethylsiloxane membranes for peripheral nerve regeneration. Microelectronic Engineering, 2014, 124, 26-29.	1.1	7
54	On cell separation with topographically engineered surfaces. Biointerphases, 2013, 8, 34.	0.6	8

#	Article	IF	CITATIONS
55	Fabrication, Operation and Flow Visualization in Surface-acoustic-wave-driven Acoustic-counterflow Microfluidics. Journal of Visualized Experiments, 2013, , .	0.2	3
56	Endothelial differentiation of mesenchymal stromal cells: when traditional biology meets mechanotransduction. Integrative Biology (United Kingdom), 2013, 5, 291-299.	0.6	22
57	Neuronal differentiation on anisotropic substrates and the influence ofÂnanotopographical noise on neurite contact guidance. Biomaterials, 2013, 34, 6027-6036.	5.7	60
58	Unveiling LOX-1 receptor interplay with nanotopography: mechanotransduction and atherosclerosis onset. Scientific Reports, 2013, 3, 1141.	1.6	20
59	Accelerated endothelial wound healing on microstructured substrates under flow. Biomaterials, 2013, 34, 1488-1497.	5.7	71
60	Easy Monitoring of Velocity Fields in Microfluidic Devices Using Spatiotemporal Image Correlation Spectroscopy. Analytical Chemistry, 2013, 85, 8080-8084.	3.2	8
61	Cell Guidance on Nanogratings: A Computational Model of the Interplay between PC12 Growth Cones and Nanostructures. PLoS ONE, 2013, 8, e70304.	1.1	21
62	Nanotopography induced contact guidance of the F11 cell line during neuronal differentiation: a neuronal model cell line for tissue scaffold development. Nanotechnology, 2012, 23, 275102.	1.3	41
63	Interaction-free, automatic, on-chip fluid routing by surface acoustic waves. Lab on A Chip, 2012, 12, 2621.	3.1	27
64	Biocompatible noisy nanotopographies with specific directionality for controlled anisotropic cell cultures. Soft Matter, 2012, 8, 1109-1119.	1.2	26
65	Control of initial endothelial spreading by topographic activation of focal adhesion kinase. Soft Matter, 2011, 7, 7313.	1.2	85
66	Nanotopographic Control of Neuronal Polarity. Nano Letters, 2011, 11, 505-511.	4.5	125
67	Nanomechanics to Drive Stem Cells in Injured Tissues: Insights from Current Research and Future Perspectives. Stem Cells and Development, 2011, 20, 561-568.	1.1	23
68	Microfluidic chip for spatially and temporally controlled biochemical gradient generation in standard cell-culture Petri dishes. Microfluidics and Nanofluidics, 2011, 11, 763-771.	1.0	7
69	Microfluidic chip with temporal and spatial concentration generation capabilities for biological applications. Microelectronic Engineering, 2011, 88, 1689-1692.	1.1	8
70	Manipulating particle trajectories with phase-control in surface acoustic wave microfluidics. Biomicrofluidics, 2011, 5, 44107-441079.	1.2	48
71	The effect of alternative neuronal differentiation pathways on PC12 cell adhesion and neurite alignment to nanogratings. Biomaterials, 2010, 31, 2565-2573.	5.7	64
72	Neuronal polarity selection by topography-induced focal adhesion control. Biomaterials, 2010, 31, 4682-4694.	5.7	107

#	Article	IF	CITATIONS
73	Surface-acoustic-wave counterflow micropumps for on-chip liquid motion control in two-dimensional microchannel arrays. Lab on A Chip, 2010, 10, 1997.	3.1	50
74	Directional PC12 Cell Migration Along Plastic Nanotracks. IEEE Transactions on Biomedical Engineering, 2009, 56, 2692-2696.	2.5	29
75	Polydimethylsiloxane–LiNbO3 surface acoustic wave micropump devices for fluid control into microchannels. Lab on A Chip, 2008, 8, 1557.	3.1	61
76	Acoustic-counterflow microfluidics by surface acoustic waves. Applied Physics Letters, 2008, 92, .	1.5	90
77	High-Resolution Poly(ethylene terephthalate) (PET) Hot Embossing at Low Temperature: Thermal, Mechanical, and Optical Analysis of Nanopatterned Films. Langmuir, 2008, 24, 12581-12586.	1.6	33
78	PC12 differentiation on biopolymer nanostructures. Nanotechnology, 2007, 18, 505103.	1.3	53
79	Acoustic charge transport in a n-i-n three terminal device. AIP Conference Proceedings, 2007, , .	0.3	0
80	Acoustic charge transport in a n-i-n three terminal device. Applied Physics Letters, 2006, 88, 212101.	1.5	5
81	Surface acoustic wave-induced electroluminescence intensity oscillation in planar light-emitting devices. Applied Physics Letters, 2005, 86, 241107.	1.5	17
82	Surface Acoustic Wave-Induced Electroluminescence Intensity Oscillation in Planar Light-Emitting Devices. Materials Research Society Symposia Proceedings, 2005, 869, 431.	0.1	2
83	Surface acoustic wave-driven planar light-emitting device. Applied Physics Letters, 2004, 85, 3020-3022.	1.5	16
84	High-performance planar light-emitting diodes. Applied Physics Letters, 2003, 82, 636-638.	1.5	23
85	Reflectionless tunneling in planar Nb/GaAs hybrid junctions. Applied Physics Letters, 2001, 78, 1772-1774.	1.5	9